Rock and Soil Mechanics

Volume 43 | Issue 3 Article 4

5-17-2022

A critical state model for structural loess considering water content

Le-le HOU
Key Laboratory for Special Area Highway Engineering of Ministry of Education, Chang'an University, Xi'an, Shaanxi 710064, China

Xiao-lin WENG
Key Laboratory for Special Area Highway Engineering of Ministry of Education, Chang'an University, Xi'an, Shaanxi 710064, China

Lin LI
Key Laboratory for Special Area Highway Engineering of Ministry of Education, Chang'an University, Xi'an, Shaanxi 710064, China

Rong-ming ZHOU
Key Laboratory for Special Area Highway Engineering of Ministry of Education, Chang'an University, Xi'an, Shaanxi 710064, China

Custom Citation

HOU Le-le, WENG Xiao-lin, LI Lin, ZHOU Rong-ming, . A critical state model for structural loess considering water content[J]. Rock and Soil Mechanics, 2022, 43(3): 737-748.

Rock and Soil Mechanics 2022 43(3): 737−748 ISSN 1000−7598
https: //doi.org/10.16285/j.rsm.2021.5995 rocksoilmech.researchcommons.org/journal

A critical state model for structural loess considering water content

HOU Le-le[1, 2], WENG Xiao-lin[1, 2], LI Lin[1, 2], ZHOU Rong-ming[1, 2]
1. School of Highway, Chang'an University, Xi'an, Shaanxi 710064, China
2. Key Laboratory for Special Area Highway Engineering of Ministry of Education, Chang'an University, Xi'an, Shaanxi 710064, China

Abstract: According to the structural evolution behaviors of undisturbed loess with different initial water contents, and based on the theory of critical-state soil mechanics, a critical-state constitutive model is proposed to describe the structural evolution and softening characteristics of undisturbed loess. The model involves stress, initial water content and strain as basic variables. By comparing the isotropic compression curves of remolded and undisturbed loess with different initial water content, the structural parameters and evolution equations of undisturbed loess with different initial water contents have been established. The model adopts the uncorrelated flow rule for plastic strain solver in terms of dilatancy equation. Nine parameters are introduced in the model, which can be calibrated from compression test and conventional triaxial shear test. Compared against the existing experimental data, it is found that this model can not only describe the influence of initial water content on the strength, deformation characteristics and failure mechanism of undisturbed loess structure, but also reasonably predict the hardening and softening characteristics of undisturbed loess. The critical state model of structural loess established in this paper provides a solution for further study of mechanical properties of loess and a theoretical basis for adequate calculation of the collapsibility and deformation of loess foundation.

Keywords: undisturbed loess; critical state theory; initial water content; structure; softening property

1 Introduction

Loess is a continental sediment in the arid and semi-arid areas of Northwest China, which forms significant characteristics of macropores, structure, and collapsibility[1]. Due to its special engineering mechanical characteristics, the action of the hydro-mechanical effect decreases strength and collapses macroporous structures, resulting in significant collapsible deformation. The abruptness, discontinuity, and irreversibility of loess collapsibility account for a series of engineering disasters such as large-area cracking, uneven settlement, main body inclination, and collapse of buildings and building foundations[1−4]. Therefore, clarifying the structural evolution law of loess under the hydro-mechanical effect and objectively describing the collapsible deformation behavior of loess are of great significance to improve the engineering construction quality and maintain the safety of geotechnical structure in loess area.

The macropore structure of undisturbed loess is formed in the process of sedimentation, and the cemented structure is built up gradually by indirect contact of particles through long-term physicochemical effects. Under the hydro-mechanical coupled effect, the connection and arrangement of soil particles are changed. The soluble salt that plays the role of cementation is dissolved to cause the cementation damage, the reduction of bonding between particles, the failure of the soil skeleton, and the collapse of macropore structure for forming the small and medium pores. These changes will lead to collapsible deformation. It is known that the structure is an intrinsic factor reflecting the mechanical properties of loess and is therefore considered to be causing an important influence on the macro deformation and mechanical properties of loess. The constitutive modeling of soil is a powerful tool to study the mechanical characteristics of soil, but it is still in the development stage up to date. Based on the compression curve of soil, Liu et al.[5−6] assumed that the deformation caused by a structure depends on plastic volume deformation and proposed a constitutive model of structural soil based on the four-dimensional space theory composed of stress state, stress history, void ratio, and structure index. Kavvadas et al.[7] constructed a model of structural soil based on the framework of the Modified Cam-Clay (MCC) model, which is suitable for remolded soil. Baudet et al.[8] investigated the relationship between the sensitivity coefficient and cementation damage and extended it to the MCC model. Zhu et al.[9] established a UH model of structural soil that involves the relationship between standard consolidation line and structural evolution. Katti et al.[10] studied the relation between remolded soil and undisturbed soil in terms of structural evolution. The disturbance state theory was proposed in their research, and the corresponding structural constitutive model was developed.

The existing structural constitutive models of soil

Received: 5 July 2021 Revised: 17 December 2021
This work was supported by the Fellowship of China Postdoctoral Science Foundation (2021M692742) and the National Natural Science Foundation of China (U1934213).
First author: HOU Le-le, male, born in 1994, PhD candidate, mainly engaged in research on loess Mechanics. E-mail: 2019021011@chd.edu.cn

are mostly introduced for clayey soils, which cannot accurately describe the structural failure in undisturbed loess. Therefore, for a comprehensive understanding of the mechanical properties of loess, it is necessary to establish corresponding constitutive models that characterize the evolution law of undisturbed loess structure. In recent years, Chen et al.[11−12], Shao et al.[13], Luo et al.[14], Xie and Qi[15], and other researchers have proposed different types of loess structural parameters based on the comprehensive potential theory, such as pore ratio, stress, strain, modulus, and structural parameters. Deng et al.[16] introduced the structural parameters of stress ratio into the MCC model on the basis of analyzing the relationship between the strength deformation characteristics and the structure of loess. Using the concept of disturbance state, Fang et al.[17] characterized the disturbance variables of soil samples by analyzing relevant CT test data. They interpreted the disturbance evolution law of structural loess and established a constitutive model of unsaturated undisturbed loess considering the evolution of mesostructure. Based on the MCC model, Zhang et al.[18] introduced structural parameters in the *p*-*q* plane to describe the structural influence of natural loess and reflected the influence on the anisotropy of natural loess by considering anisotropic parameters introduced by the rotation of the yield surface. Finally, an MCC model was established considering the influence of loess structure and anisotropy. The constitutive models introduced above characterized the structure's impact on the deformation of loess. However, these studies do not consider the influence of initial water content on undisturbed loess's structure and deformation characteristics. The structural strength and deformation characteristics of undisturbed loess are highly related to the initial water content compared with remolded loess[19−20]. Discussing the influence of initial water content and load on the structural evolution of loess is the best choice to describe the mechanical properties of undisturbed loess. In addition, the MCC model, which provides the dominant framework of the current models, cannot reflect the structural characteristics of the undisturbed loess. Therefore, the establishment of a constitutive model containing limited parameters with clear physical meaning, which describe the influence of initial water content on the structure and softening characteristics of undisturbed loess, has good engineering application prospects and theoretical significance. Based on the research work of the above relevant scholars, within the framework of plastic mechanics and critical state theory, this paper focuses on the influence of initial water content on the structural evolution law of loess and puts forward an elastic-plastic model that describes the structural evolution law and softening characteristics of undisturbed loess. The validation of the model is carried out by comparing the predicted results against the test data from relevant literature.

2 Loess compression equation considering the influence of structure

The pore structure of undisturbed loess is damaged under the influence of load and moisture. In this process, the large pores gradually collapse into medium and small pores, resulting in the structural deterioration of loess until complete damage. The remolded loess is known as the form when the structure of the loess is completely destroyed, which is also defined as 'structure lost'. Therefore, the influence of the structure of undisturbed loess on its mechanical properties can be investigated by comparing that of remolded loess under the same conditions for all stress paths. The isotropic compression curves of these loess forms under ideal conditions are shown in Fig.1, where e and e^* are the void ratio of undisturbed loess and remolded loess, respectively. For easy illustration, the following * is expressed as the remolded loess parameter. The p is the mean stress applied on undisturbed loess in the test; the p_s is the initial yield stress of undisturbed loess; the Δe is the additional void ratio mobilized by the structure of undisturbed loess under stress ($p > p_s$); and the Δe_i is the corresponding value for the initial yield stress, which reflects the initial structural strength of undisturbed loess. The compression curves of undisturbed loess and remolded loess coincide when $\Delta e = 0$. In this condition, undisturbed loess degrades into remolded loess and has lost structure. Therefore, the change of void ratio under isotropic compression of undisturbed loess can be expressed as Eq.(1).

$$e = e^* + \Delta e \tag{1}$$

In order to simulate the decrease of additional void

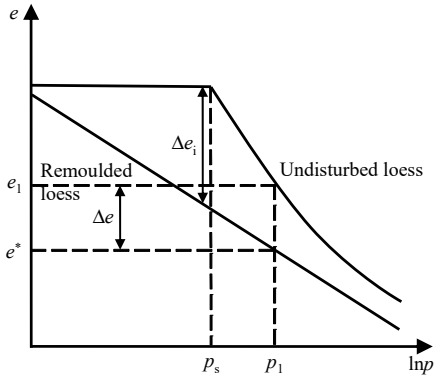

Fig. 1 Isotropic compression curves of remolded loess and undisturbed loess

ratio induced by the increase of stress in undisturbed loess under isotropic compression ($p > p_s$), the following equation is used to describe the compression characteristics of loess[5]:

$$\Delta e = \Delta e_i \left(\frac{p_s}{p} \right)^b \tag{2}$$

where b is the damage index of loess structure, which represents the change of the initial structure of loess with the initial water content of soil. The b decreases and the corresponding structural failure rate also decreases with the increase of the initial water content.

3 Structural evolution law of undisturbed loess

In the process of sedimentary formation, undisturbed loess forms obvious structural characteristics after the history of hydro-mechanical effect, which builds up great structural strength. The greater initial yield stress of undisturbed loess is obtained under the stronger initial structure. The damage to the loess structure shows an obvious difference in deformation characteristics. For example, the soil with a strong initial structure has a stronger deformation capacity after the damage. Therefore, the deformation characteristics of undisturbed loess structure after strength failure, as well as mechanical properties, are determined by its initial structure. Correctly describing the structural evolution law of loess is the key to establishing the constitutive model of structural loess. As mentioned above, the influence of initial moisture content on the structure of loess has been a consensus in the industry. The higher value results in easier damage to the initial structure of the soil and lower structural strength and deformation rate of undisturbed loess with the same initial void ratio. In order to simplify the study of the impact of initial water content on loess structure, this paper indirectly reflects the strength of initial loess structure by establishing the relationship between initial loess structure and initial water content; and the structural attenuation under the hydro-mechanical effect is directly reflected by parameter b. Therefore, the initial yield stress, initial additional void ratio, and damage index b of loess structure are defined as state variables, which are dependent on the initial water content w. Therefore, Eq.(2) can be re-expressed as

$$\Delta e = \Delta e_i(w) \left(\frac{p_s(w)}{p} \right)^{b(w)} \tag{3}$$

where $p_s(w)$, $\Delta e_i(w)$, and $b(w)$ are the initial yield stress, initial additional void ratio, and damage index related to the initial water content, respectively. For the convenience of explanation, these parameters in the following paragraphs are expressed as initial yield stress p_s, initial additional void ratio Δe_i, and damage index b. Figure 2 shows the compression curve of undisturbed loess under different initial moisture content. It is worth noting that since the initial water content also has an impact on the deformation characteristics of remolded loess, the corresponding compression lines under different initial water content in Fig.2 do not coincide.

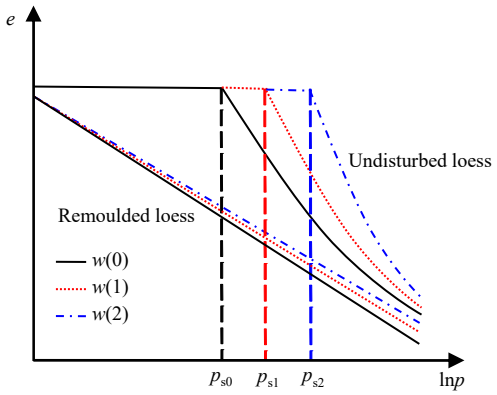

Fig. 2 Compression curves of remolded loess and undisturbed loess with different initial water contents

3.1 Relationship between initial yield stress and initial water content

Zhang et al.[18] carried out the one-dimensional compression tests of remolded loess and undisturbed loess under the same water content and determined the p_s under different initial water content by using the traditional Casagrande method. Since the results are consistent with those of the isotropic compression test, the variation law of undisturbed loess in isotropic stress space is therefore characterized by the one-dimensional compression results[21−22]. Figure 3 shows the one-dimensional compression consolidation test results of Xi'an Q_3 undisturbed loess with different initial water content[18]. It can be seen that the lower initial water content leads to greater initial yield stress for the undisturbed loess. The approximate exponential relation between the two factors can be found. With the increase of the initial water content, the initial yield stress shows a rapid reduction firstly and then decreases at a relatively stable gradient. Therefore, the relationship between the initial water content and the initial yield stress of loess can be approximately fitted as an exponential function:

$$p_s = me^{nw} \tag{4}$$

where m and n are fitting parameters. For investigating the influence of fitting parameters on the initial yield stress of simulated undisturbed loess, the parametric study is shown in Fig.4. It can be seen that the m mainly affects the initial yield stress at low water content, whereas the

n has a significant effect on the initial yield stress in the whole range of water content. The larger value of m and n results in the greater initial yield stress and the corresponding failure rate of the structure.

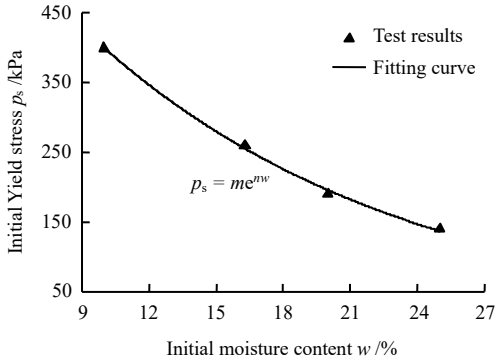

Fig. 3 Initial yield stress of undisturbed loess with different initial water contents

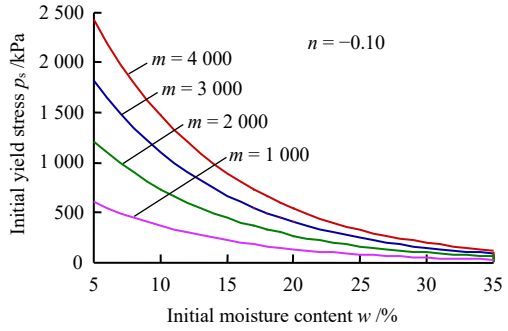

(a) Influence analysis of m

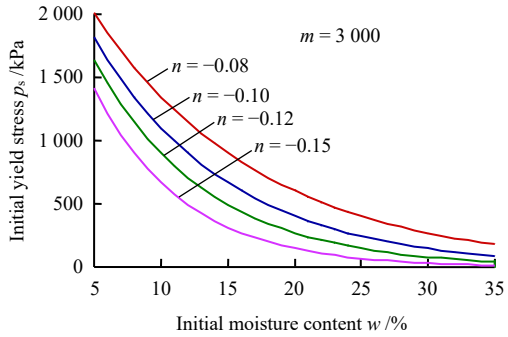

(b) Influence analysis of n

Fig. 4 Influence of fitting parameters on the initial yield stress of loess

3.2 Relationship between initial additional void ratio and initial water content

By comparing the difference in void ratio between undisturbed loess and remolded loess under the initial yield stress corresponding to undisturbed loess, the relationship between the initial additional void ratio and the initial water content of undisturbed loess is determined. Table 1 shows the additional void ratio under different initial water content obtained from the literature [18], and the fitting curve is shown in Fig.5. It can be seen that w has a significant impact on the Δe_i. The initial additional void ratio of undisturbed loess decreases with the increase of initial water content. The two variables basically follow a linear relationship, expressed as

$$\Delta e_i = \alpha + \beta w \tag{5}$$

where α and β are fitting parameters. The α represents the size of the initial additional pore ratio of undisturbed loess under low water content, and the greater value increases Δe_i, resulting in a more significant pore structure of loess and the stronger corresponding deformation capacity. The β reflects the change rate of the additional void ratio of undisturbed loess with initial water content. The greater β means that the smaller the effect of initial water content on the initial additional void ratio.

Table 1 Initial additional voids ratio of undisturbed loess with different initial water content

Initial moisture content w /%	Initial additional void ratio Δe_i
10.0	0.353
16.3	0.330
20.0	0.305
25.0	0.260

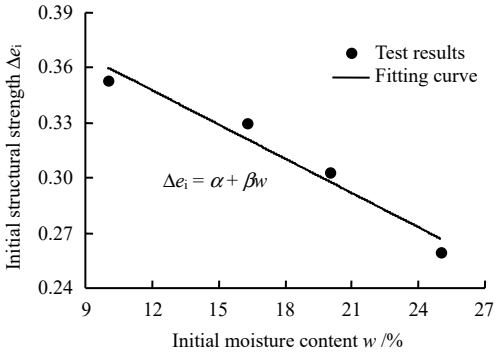

Fig. 5 Initial structural strength of undisturbed loess with different initial water contents

3.3 Relationship between structure deterioration index and initial water content

The structural damage index b of undisturbed loess after yielding through Eq.(2) is calculated from the test results. Take P as 300, 400, and 500 kPa as the reference stress point, and use the average value of three calculations to obtain the corresponding damage index, as shown in Fig.6. It can be seen that the relationship between the initial moisture content of undisturbed loess and its structural deterioration index can be approximately fitted as a line expressed as

$$b = c + dw \tag{6}$$

where c and d are fitting parameters similar to α and β. Compared with strong structural loess, weak samples

cause less deformation before structural damage. The soil deformation develops slowly after the structural damage, showing weaker deformation capacity and smaller corresponding damage index compared to strong structural loess.

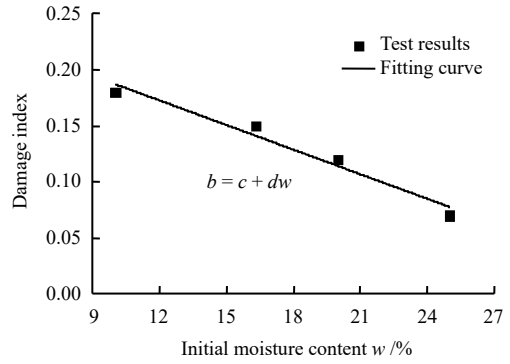

Fig. 6 Damage index of undisturbed loess with different initial water contents

4 Constitutive model of undisturbed loess based on critical state

4.1 Yield surface

Based on the assumption that remolded loess does not have 'Structure', the MCC model is used to describe the stress-strain relationship of remolded loess. This study *adopts* the elliptical yield surface of undisturbed loess, which is similar to the MCC model. The two endpoints are the coordinate origin and the initial yield stress of remolded loess p_0 and the initial yield stress of undisturbed loess p_s (see Fig.7). In the shearing stage of undisturbed loess, the soil gradually deforms with the increase of p. When p is greater than the initial yield stress of undisturbed loess, the structure is damaged, and the soil is significantly deformed. Compared with remolded loess, the difference between p_s and p_0 indicates the influence of structure on the initial yield stress of loess due to the existence of structure. Referring to the expression of the MCC model yield surface constitutive model[23], the yield equation f of undisturbed loess can be expressed as

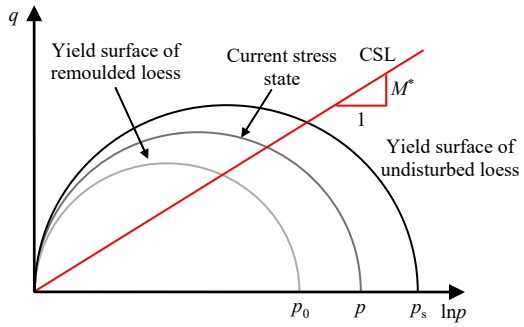

Fig. 7 Yield surfaces of undisturbed loess and remolded loess

$$f = q^2 - M^{*2} p\left(p_s - p\right) \tag{7}$$

where M^* is the critical state stress ratio of remolded loess, and q is partial stress.

4.2 Volume strain law under general stress path

As shown in Fig.2, the slopes of elastic and plastic parts of remolded loess in the plane of $e-\ln p$ are κ^* and λ^*, respectively, and the normal consolidation curve equation under isotropic compression can be expressed as

$$e^* = e_0^* - \lambda^* \ln p \tag{8}$$

The hardening parameters of undisturbed loess, following the assumption in the MCC model, are dependent on the plastic volumetric strain. The yield surface of undisturbed loess can be represented by all stress states with the same plastic volumetric strain. Therefore, the plastic volumetric strain is only determined by the change in yield surface size. Combining Eqs.(1), (3), and (8), the variation law of void ratio of undisturbed loess is obtained:

$$e = e_0^* + \Delta e_{\mathrm{i}}(w)\left(\frac{p_s(w)}{p}\right)^{b(w)} - \lambda^* \ln p \tag{9}$$

The incremental form of the total volume strain of undisturbed loess under the general stress path can be obtained by differentiating Eq.(9) and combining Eq.(3), i.e.,

$$\mathrm{d}\varepsilon_{\mathrm{v}} = \kappa^* \frac{\mathrm{d}p}{(1+e)\,p} + \left(\lambda^* - \kappa^* + b\Delta e\right)\frac{\mathrm{d}p_s}{(1+e)\,p_s} \tag{10}$$

where ε_{v} is volumetric strain.

The first term on the right of Eq.(10) is elastic volumetric strain, which follows the same form as the calculation of the MCC model. The last term is plastic volumetric strain. Considering the influence of the shear mechanism on deformation, it is assumed that structural failure and plastic volumetric strain depend on the size of the yield surface and current shear stress level. Therefore, it is extended as

$$\mathrm{d}\varepsilon_{\mathrm{v}}^{\mathrm{p}} = \left[\lambda^* - \kappa^* + b\Delta e\left(1 + \frac{\eta}{M^* - \eta}\right)\right]\frac{\mathrm{d}p_s}{(1+e)\,p_s} \tag{11}$$

where $\varepsilon_{\mathrm{v}}^{\mathrm{p}}$ is the plastic volumetric strain, and η is the stress ratio ($\eta = q/p$)

4.3 Flow rule

In this paper, the non-associated flow law is adopted to describe the non-associated characteristics of undisturbed loess utilizing the dilatancy equation, and the tensor expression of plastic strain increment is obtained:

$$\mathrm{d}\varepsilon_{\mathrm{v}}^{\mathrm{p}} = \Lambda\frac{\partial g_{\mathrm{LC}}}{\partial \boldsymbol{\sigma}_{ij}} = \Lambda\left(\frac{\partial g_{\mathrm{LC}}}{\partial p}\frac{\partial p}{\partial \boldsymbol{\sigma}_{ij}} + \frac{\partial g_{\mathrm{LC}}}{\partial q}\frac{\partial q}{\partial \boldsymbol{\sigma}_{ij}}\right) \tag{12}$$

where Λ is the plasticity factor, indicating the increment of plastic strain; g_{LC} is plastic potential function; and $\boldsymbol{\sigma}_{ij}$ is the tensor expression of stress in three-dimensional stress space. It is worth noting that there is no specific expression of g_{LC} in this paper, which only serves for subsequent equation derivation.

Considering the influence of undisturbed loess structure on the flow rule, based on the MCC model framework, the parameter ω describing the influence of soil structure on plastic deviatoric strain increment is introduced, and the undisturbed loess dilatancy equation is obtained:

$$\frac{\mathrm{d}\varepsilon_{\mathrm{d}}^{\mathrm{p}}}{\mathrm{d}\varepsilon_{\mathrm{v}}^{\mathrm{p}}}=\frac{\Lambda\dfrac{\partial g_{\mathrm{LC}}}{\partial q}}{\Lambda\dfrac{\partial g_{\mathrm{LC}}}{\partial p}}=\frac{\Lambda\dfrac{\partial f}{\partial q}(1-\omega\Delta e)}{\Lambda\dfrac{\partial f}{\partial p}}=\frac{2\eta(1-\omega\Delta e)}{M^{*2}-\eta^2} \tag{13}$$

where $\varepsilon_{\mathrm{d}}^{\mathrm{p}}$ is the deviatoric strain. ω is the positive and the direction of plastic strain increment is toward the yield surface. Hence,

$$0\leqslant\omega\leqslant\frac{1}{\Delta e_{\mathrm{i}}} \tag{14}$$

4.4 Stress-strain relationship

According to the elastic-plastic theory, the total strain increment $\mathrm{d}\boldsymbol{\varepsilon}_{ij}$ is decomposed as the sum of elastic strain increment and plastic strain increment:

$$\mathrm{d}\boldsymbol{\varepsilon}_{ij}=\mathrm{d}\boldsymbol{\varepsilon}_{ij}^{\mathrm{e}}+\mathrm{d}\boldsymbol{\varepsilon}_{ij}^{\mathrm{p}} \tag{15}$$

4.4.1 Elastic strain increment

The increment of elastic strain can be calculated by general Hooke's law and is expressed as

$$\mathrm{d}\boldsymbol{\varepsilon}_{ij}^{\mathrm{e}}=\frac{1+\mu^*}{E}\mathrm{d}\boldsymbol{\sigma}_{ij}-\frac{\mu^*}{E}\boldsymbol{\delta}_{ij}\mathrm{d}\boldsymbol{\sigma}_{ij} \tag{16}$$

where μ^* is the Poisson's ratio of remolded loess; $\boldsymbol{\delta}_{ij}$ is the Kronecker symbol (when $i=j$, $\boldsymbol{\delta}_{ij}=1$; when $i\neq j$, $\boldsymbol{\delta}_{ij}=0$); and E is Young's modulus, which is expressed as

$$E=\frac{3(1-2\mu^*)(1+e)\,p}{\kappa^*} \tag{17}$$

4.4.2 Plastic strain increment

The plastic strain increment is derived by the non-associated flow rule (Eq.(12)). The plasticity factor can be obtained by solving the consistency of the yield equation f:

$$\frac{\partial f}{\partial p}\mathrm{d}p+\frac{\partial f}{\partial q}\mathrm{d}q+\frac{\partial f}{\partial p_{\mathrm{s}}}\mathrm{d}p_{\mathrm{s}}=0 \tag{18}$$

where the differential of yield equation f to spherical stress and partial stress is obtained as

$$\frac{\partial f}{\partial p}=p\left(M^{*2}-\eta^2\right) \tag{19}$$

$$\frac{\partial f}{\partial q}=2q \tag{20}$$

Differentiate the yield equation f with respect to the initial yield stress to obtain

$$\frac{\partial f}{\partial p_{\mathrm{s}}}=-M^{*2}p \tag{21}$$

Substituting the plastic volumetric strain increment expressed by the non-associated flow rule (Eq.(12)) into Eq.(21), the expression of the plasticity factor Λ can be obtained:

$$\Lambda=-\frac{\dfrac{\partial f}{\partial p}\mathrm{d}p+\dfrac{\partial f}{\partial q}\mathrm{d}q}{\dfrac{\partial f}{\partial p_{\mathrm{s}}}\dfrac{\partial p_{\mathrm{s}}}{\partial\varepsilon_{\mathrm{v}}^{\mathrm{p}}}\dfrac{\partial f}{\partial p}} \tag{22}$$

By combining Eqs.(7), (19), (20), and (21), the specific expression of the plasticity factor Λ can be obtained as

$$\Lambda=\frac{\left(\lambda^*-\kappa^*\right)\left(M^*-\eta\right)+b\Delta eM^*}{(1+e)\left(M^*-\eta\right)}\frac{\left(\mathrm{d}p+\dfrac{2\eta\mathrm{d}q}{M^{*2}-\eta^2}\right)}{M^{*2}p^2+q^2} \tag{23}$$

Substituting Eq.(23) into Eq.(12), the specific tensor expression of plastic strain increment can be obtained after sorting as follows:

$$\mathrm{d}\boldsymbol{\varepsilon}_{ij}^{\mathrm{p}}=\frac{\left(\lambda^*-\kappa^*\right)\left(M^*-\eta\right)+b\Delta eM^*}{(1+e)\left(M^*-\eta\right)}\frac{\left(\mathrm{d}p+\dfrac{2\eta\mathrm{d}q}{M^{*2}-\eta^2}\right)}{M^{*2}p^2+q^2}\cdot\left[\frac{p\left(M^{*2}-\eta^2\right)}{3}\boldsymbol{\delta}_{ij}+3\left(\boldsymbol{\sigma}_{ij}-p\boldsymbol{\delta}_{ij}\right)(1-\omega\Delta e)\right] \tag{24}$$

When the structure of undisturbed loess is not considered (ω= 0; Δe = 0), Eq.(24) is reduced to the plastic strain increment expression of the MCC model. Therefore, the MCC model can be regarded as a special case of this model.

4.5 Softening rule

Undisturbed loess has significant softening and dilatancy characteristics as widely known by scholars[11, 24−25]. The undisturbed loess can be regarded as elastic material when the stress state is located in the yield surface. The plastic deformation occurs gradually when the current stress state increases to the initial yield surface. The softening occurs when the soil reaches the initial yield surface and meets the boundary conditions, satisfying $M^*<\eta$ [10]. In this process, the structure of loess is gradually destroyed, and the yield surface shrinks. It is assumed that the size of the yield surface is still determined

by the current stress state. In this condition, the yield surface of undisturbed loess gradually shrinks until the current stress ratio decreases to M^*, at which time the structure of undisturbed loess will be completely lost. Therefore, the softening behavior of undisturbed loess can still be described by the initial yield equation.

Equation (11) represents the change of plastic volumetric strain during deformation. This study calculates the plastic volumetric strain increment in the softening process based on Eq.(11) for simplification. Considering that the shrinkage of the yield surface ($\mathrm{d}p_s$ is negative), when the additional void ratio corresponding to the initial yield stress is positive, the volumetric strain caused by the structure becomes negative, which leads to the unrealistic increase of the additional void ratio caused by the undisturbed loess structure in the softening process. Therefore, the expression of plastic deviatoric strain increment $\mathrm{d}\varepsilon_{\mathrm{d}}^{\mathrm{p}}$ should be modified. The influence of the additional void ratio is considered in the calculation, and Eq.(11) is modified to adapt to the softening characteristics of structural loess:

$$\mathrm{d}\varepsilon_{\mathrm{d}}^{\mathrm{p}}=\frac{2\eta(1-\omega\Delta e)}{M^{*2}-\eta^2}\frac{\left(\lambda^*-\kappa^*\right)-b\Delta eM^*}{(1+e)\left(M^*-\eta\right)}\frac{\mathrm{d}p_{\mathrm{s}}}{p_{\mathrm{s}}} \tag{25}$$

The above expression characterizing the loess softening only changes the symbol of the relationship between $\mathrm{d}\varepsilon_{\mathrm{d}}^{\mathrm{p}}$ and the void ratio caused by structural failure. Therefore, the direction of strain increment is outward the yield surface. The strain-softening characteristics of structural loess $\mathrm{d}\boldsymbol{\varepsilon}_{ij}^{\mathrm{e}}$ and $\mathrm{d}\varepsilon_{\mathrm{v}}^{\mathrm{p}}$ are still calculated based on Eqs.(11) and (16). $\mathrm{d}\varepsilon_{\mathrm{d}}^{\mathrm{p}}$ is calculated using Eq.(25). Therefore, the strain increment in the softening process is determined.

4.6 Determination of the parameters

There are nine parameters in the model, which can be determined directly through the test or the fitting of the relevant test results. The e_0^* and μ^* are determined by porosity meter, compression test, and other tests. The λ^* and κ^* are the MCC model parameters, which can be determined by one-dimensional compression or isotropic compression test. The structural parameters p_{s}, Δe_{i}, and b are determined by the comparison of the isotropic compression test of undisturbed loess and remolded loess. The initial moisture content w is determined by the drying method. The fitting parameters m, n, α, β, c, and d between the initial moisture content and structural parameters are calibrated against isotropic compression test results; M^* and ω are determined by conventional triaxial test under different initial moisture content.

5 Model validation

The validation of the model established in this study in the description of structural evolution law and strain softening characteristics is completed by the simulation performed on the conventional triaxial shear test results of unsaturated undisturbed loess in typical loess areas. The prediction function of the constitutive model is realized using MATLAB numerical tool.

5.1 Simulation of undisturbed loess compression test

Literature[18] carried out compression tests under different initial moisture contents for Xi'an undisturbed loess. The model parameters are determined by using the test data published in document[18], as shown in Table 2. The compression test simulation of undisturbed loess samples under different initial moisture content is carried out. The prediction results and test comparison of the model are shown in Fig.8.

Table 2 Calculation parameters of undisturbed loess compression test

Parameters	λ^*	κ^*	μ^*	M^*	e_0^*	α
Value	0.17	0. 031	0.33	1.4	1.095	0.422
Parameters	β	m	n	c	d	
Value	−0.006	817.5	−0.071	0.26	−0.007 3	

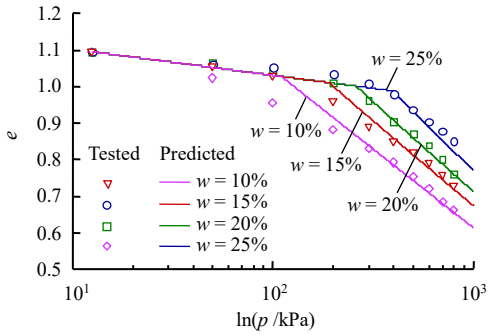

Fig. 8 Simulation of compression tests on undisturbed loess

It can be seen from figure 8 that the model achieves a good representation of the general procedure in the compression process of undisturbed loess. The greater initial pore water content leads to higher initial yield stress and a lower deformation rate in post yielding stage. That is basically consistent with the test results. Due to a certain under consolidation in the process of historical deposition in the structural loess, the smaller initial water content causes greater influence by historical deposition. Therefore, the elastic deformation in the initial stage of the test is determined to be small. The influence of initial water content is not considered as one of the model parameters in this research, which may lead to the deviation of

simulation results, although the overall fitting results have good agreement.

5.2 Simulation of consolidated drained triaxial shear test of saturated undisturbed loess

In reference [26], the consolidated drained triaxial shear test of undisturbed loess in a saturated state was carried out for the undisturbed loess in the Jingyang area, and the effects of different confining pressures on the structural failure and deformation characteristics of loess were analyzed. The stress loading path is shown in Fig.9. In this research, the test results under confining pressures of 200, 300 and 400 kPa are selected as data cases. Model parameters are set up as $\lambda^* = 0.101$, $\kappa^* = 0.014$, $\mu^* = 0.31$, $M^* = 1.42$, $e_0^* = 0.68$, $\omega = 0.2$, $p_s = 680$ kPa, $b = 0.3$, and $\Delta e_i = 0.15$. The MCC model parameters λ^*, κ^*, M^*, p_s, Δe_i, and b are determined by the isotropic compression test of saturated remolded loess and saturated undisturbed loess carried out in document[26]. ω is obtained by back analysis. The predicted results of the model are shown in Fig.10.

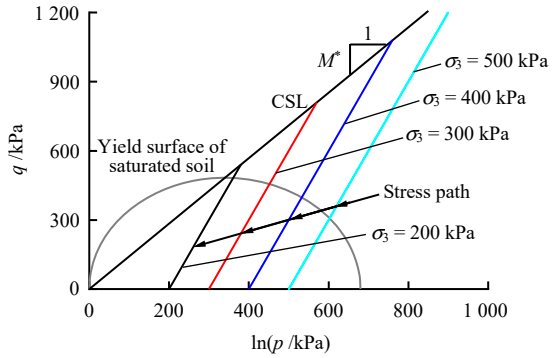

Fig. 9 Loading path of saturated undisturbed loess in triaxial tests

It can be seen from Fig.10 that the predicted results of the model are generally consistent with the test results. There is an obvious strain turning point in the curve of the relationship between axial strain and deviatoric stress of loess under large confining pressure, showing the characteristics of obvious strain hardening that becomes less significant with the decrease of confining pressure. The model has good agreement with the test results when simulating the deformation characteristics of saturated undisturbed loess under high confining pressure, whereas the low confining pressure causes a certain deviation from the test results. This is reasonable since, in the test process, the soil structure of samples with different initial moisture content is damaged to varying degrees due to different consolidation stress. However, the corresponding structure cannot be identified accurately in this process. Only the initial structure can be assumed, resulting in the error between test results and predicted values on the deformation of loess under low consolidation confining pressure.

5.3 Triaxial shear test simulation of consolidated drained undisturbed loess

In reference [27], the drained triaxial shear test of undisturbed loess under different initial moisture contents was carried out for the undisturbed loess in the Qingyang area, and the effects of different initial moisture content on the structural failure and deformation characteristics of loess were studied. The stress loading path is shown in Fig.11.

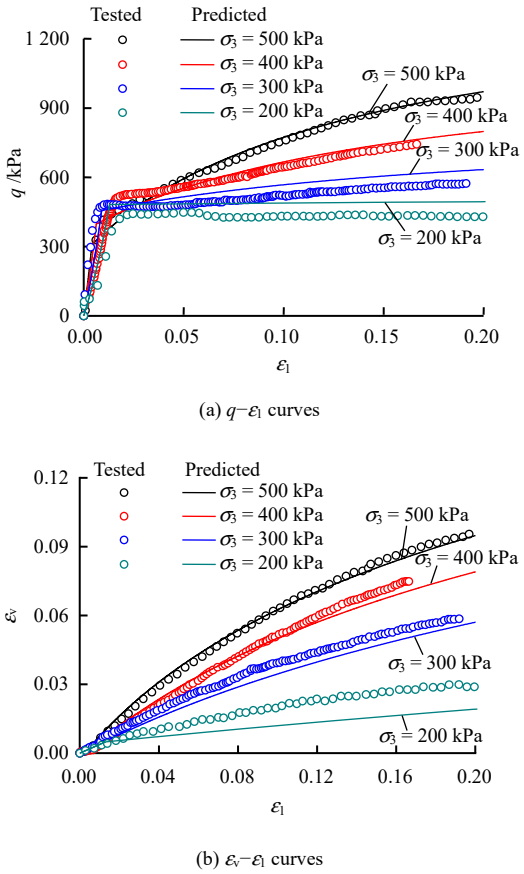

Fig. 10 Prediction of saturated undisturbed loess in triaxial tests

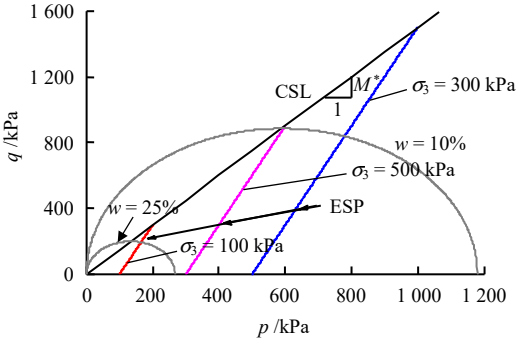

Fig. 11 Loading stress path of undisturbed loess in triaxial tests

In this study, the triaxial test results with the initial

moisture content of 10% and 25% are selected as the cases. Since the consolidated drained triaxial shear test is only carried out for the undisturbed loess under different initial moisture content and confining pressure, some model parameters cannot be obtained directly. In this study, the initial moisture content of 10% and the confining pressure of 300 kPa are employed as the basis for parameter calibration. Referring to the relevant test results, the model parameters are determined as $\lambda^* = 0.17$, $\kappa^* = 0.01$, $\mu^* = 0.3$, $M^* = 1.473$, $e_0^* = 0.901$, $\omega = 1$, $\alpha = 0.708$, $\beta = -0.011$, $m = 2\ 510$, $n = -0.091$, $c = 0.607$, and $d = -0.11$. The predicted results are shown in Fig.12.

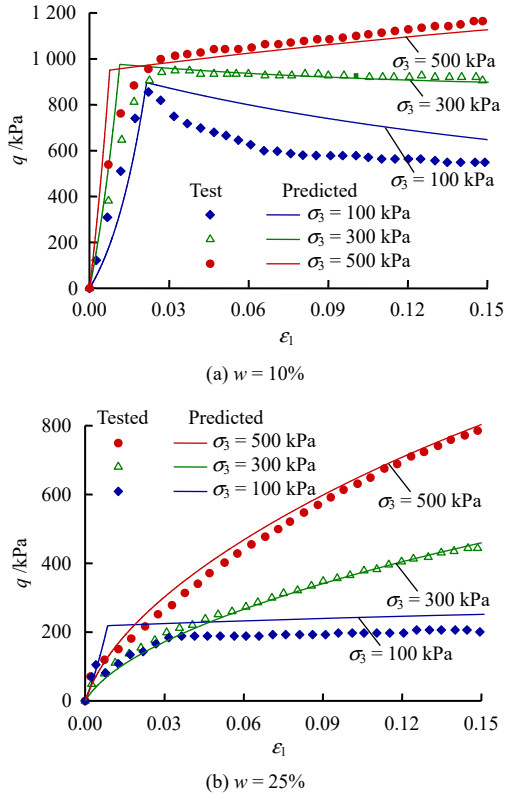

Fig. 12 Simulation of triaxial tests on loess in the Qingyang area

It can be seen from Fig.12 that the prediction results of the model are generally consistent with the test results. When the initial water content is small, there is an obvious strain turning point in the curve of the relationship between axial strain and deviatoric stress of loess, and there is obvious strain softening and strain hardening under low confining pressure and high confining pressure, respectively. The saturated soil leads to the increase of axial strain with deviatoric stress, showing strain hardening. The larger the consolidation confining pressure, the faster the deformation rate. The model is more consistent with the test results when simulating the deformation characteristics of undisturbed loess under high confining pressure. The low confining pressure behaves as softening characteristics, but there is an error with the test results. This is reasonable since that in the test process, the soil structure of samples with different initial moisture content is damaged to varying degrees due to different consolidation stress. However, the corresponding structure cannot be identified accurately in this process. Only the initial structure can be assumed, resulting in the error between test results and predicted values on the deformation of loess under low consolidation confining pressure.

6 Model analysis

The model is employed to analyze the structural evolution law and deformation characteristics of loess under different initial water contents to quantify the influence of initial water content on the mechanical properties of loess. The basic parameters of the material are shown in Table 3. The initial stress states are $p = 100$ kPa and $q = 0$ kPa. The stress loading path is shown in Fig.9.

Table 3 Calculation parameters of undisturbed loess triaxial test

Parameters	λ^*	κ^*	μ^*	M^*	e_0^*	ω
Value	0.17	0. 01	0.33	1.473	0.901	0.4
Parameters	α	β	m	n	c	d
Value	0.833	−0.023	3 175	−0.099	0.667	−0.017

6.1 Analysis of initial yield stress p_s of loes

Figure 13 shows the influence of initial yield stress on yield surface and deformation characteristics when the initial moisture content is 5%, 10%, 15%, 20%, and 25%, respectively. The influence of initial moisture content w on Δe_i and b is not considered (fixed values: $\Delta e_i = 0.4$ and $b = 0.45$). Figure 9 shows that the higher initial water content leads to the smaller initial yield stress of undisturbed loess and the corresponding yield surface. The initial water content of close to 20% drives the loess strain softening, which weakens with the increase of water content until at a certain water content. The soil changes from strain softening to strain hardening. In addition, the peak strength of undisturbed loess is not only related to the current structure but also depends on the initial stress state, initial void ratio, and stress loading path. Regardless of strain hardening or softening, the peak strength of undisturbed loess finally tends to its corresponding strength in a critical state. The shear process of structural loess is mainly characterized by shrinkage. Under the tested initial moisture content, the shear dilation characteristics of loess have not been represented since this phenomenon may occur only when

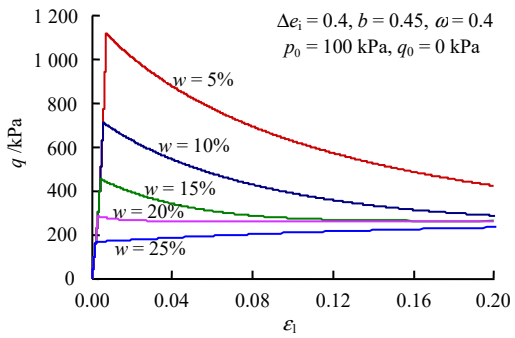

(a) Relationship between deviatoric stress q and axial strain ε_1

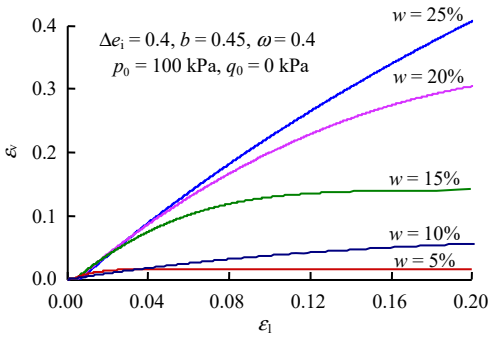

(b) Relationship between volumetric strain ε_v and axial strain ε_1

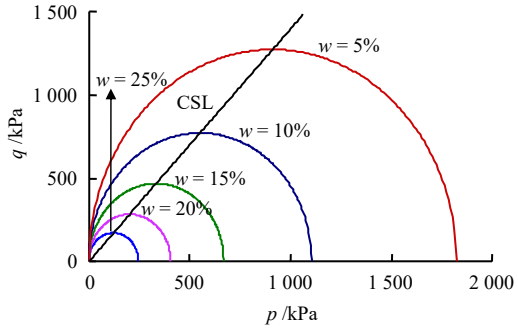

(c) Yield surface under different initial moisture contents

Fig. 13 Analysis of initial yield stress p_s of undisturbed loess

the initial moisture content is very small ($w < 5\%$).

6.2 Analysis of initial additional void ratio Δe_i of loess

Figure 14 shows the influence of the initial additional void ratio on the deformation characteristics of loess when the initial water content is 5%, 10%, 15%, 20%, and 25%, respectively. The influence of initial water content w on p_s and b is not considered (fixed values: $p_s = 300$ kPa and $b = 0.4$). As shown in Fig.13, the increase of initial moisture content results in a faster axial strain rate and soil comes to a critical state earlier. Comparing the effects of different initial additional void ratio on the stress-strain relationship of undisturbed loess, the results show that the change of the maximum additional void ratio caused by initial water content has no significant effect on loess deformation from the view of the whole process.

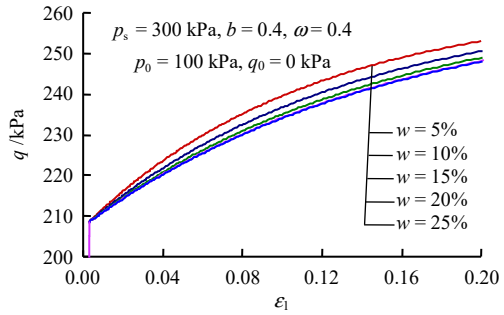

(a) Relationship between deviatoric stress q and axial strain ε_1

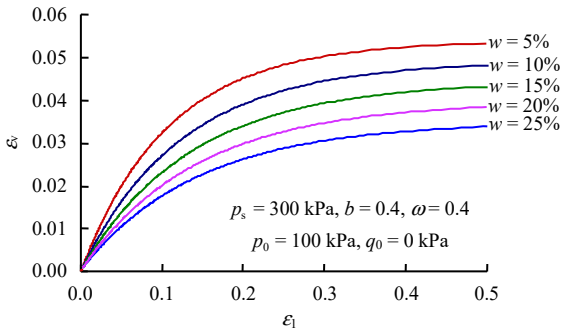

(b) Relationship between volumetric strain ε_v and axial strain ε_1

Fig. 14 Analysis of additional void ratio Δe_i of undisturbed loess

6.3 Analysis of structural damage index b of loess

Figure 15 shows the influence of the structural damage index of undisturbed loess on its deformation characteristics when the initial water content are 5%, 10%, 15%, 20%, and 25%, respectively. The influence of initial water content w on p_s and Δe_i is not considered (fixed values: $p_s = 200$ kPa and $\Delta e_i = 0.4$). It can be seen from Fig.15(a) that under the isotropic compressive stress path, without considering the influence of the initial additional void ratio, the smaller initial water content leads to the smaller the additional void ratio and faster failure rate of loess structure. The soil finally reaches the critical state.

The reproduction of shear characteristics of structural loess with different structural damage index b is shown in Fig.15(b) and 15(c). The results show that the final state of structural loess under shear stress is independent of its structure but only dominated by the critical stress state. The structure of undisturbed loess disappears completely at a critical state, and the smaller initial moisture content leads to faster failure. The consistent stress path, initial void ratio, initial additional void ratio, and stress state result in an identical value of the final deviatoric stress and volumetric strain. Therefore, adjusting parameter b does not affect the final state of loess.

6.4 Analysis of loess strain parameter ω

Figure 16 shows the simulation results of the triaxial shear tests of undisturbed loess when the strain parameter

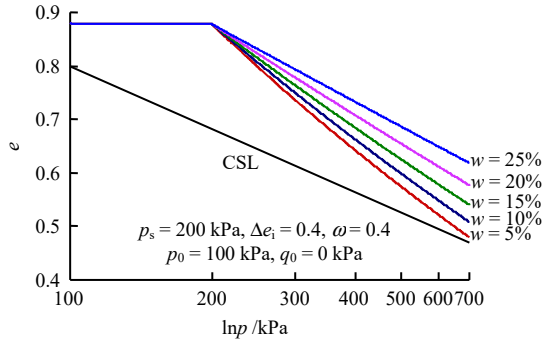

(a) isotropic compression curve

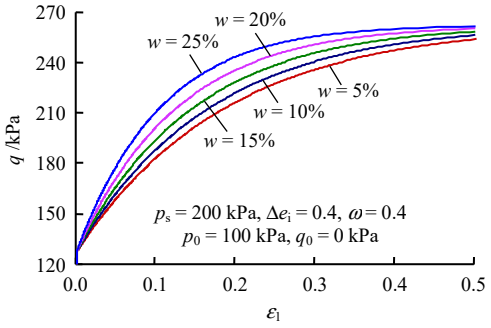

(b) relationship between deviatoric stress q and axial strain ε_1

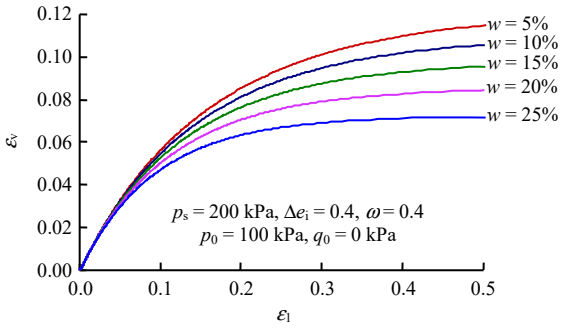

(c) relationship between volumetric strain ε_v and axial strain ε_1

Fig. 15 Analysis of initial additional porosity ratio b of undisturbed loess

ω values are 0.3, 1.0, 2.0, 3.0, and 5.0, respectively. In order to analyze the influence on the deformation characteristics of loess, the change of initial water content is not considered (fixed values: $p_s = 200$ kPa, $\Delta e_i = 0.2$, and $b = 0.2$). It can be seen from the figure that the ω value has a significant impact on the stress-strain relationship of loess. The larger ω leads to a faster plastic deformation rate and the earlier failure. Under the same initial moisture content, the ω value only affects the deformation process but is irrelevant to the final state of loess.

7 Conclusions

(1) The MCC model is extended in this study. The proposed model considers the changes in mechanical

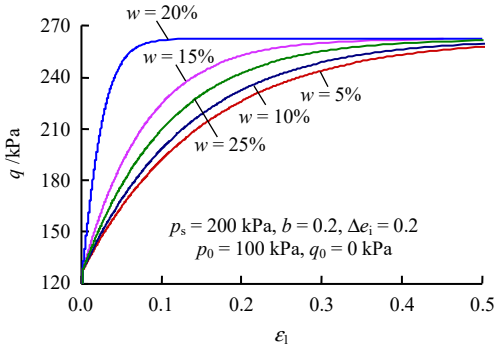

(a) Relationship between deviatoric stress q and axial strain ε_1

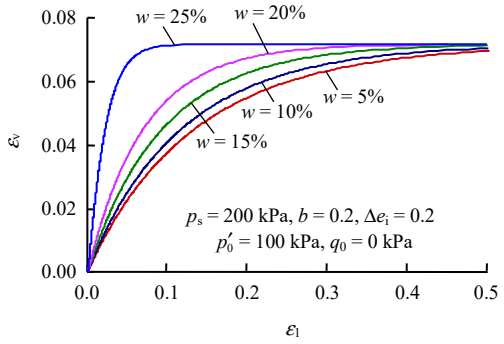

(b) Relationship between volumetric strain ε_v and axial strain ε_1

Fig. 16 Analysis of strain parameter ω of undisturbed loess

properties of undisturbed loess due to the different structures caused by different initial moisture content. In addition to the five basic parameters of the original MCC model, the modified model introduces the initial structural parameter p_s, which is affected by the initial water content, the initial additional void ratio Δe_i, the structural damage index b, and the strain parameter ω.

(2) Based on the analysis of existing relevant experimental research, this paper focuses on the impact of initial water content on loess structure and stress-strain relationship and establishes the quantitative relationship between initial water content and loess structural parameters.

(3) The structural evolution law of undisturbed loess in $e - \ln p$ space is described by considering the influence of initial water content on loess structure. Referring to the relationship between stress ratio η and critical state stress ratio M^*, a stress dilatancy equation is proposed to describe the strain hardening and softening characteristics of loess. Moreover, a critical state model of structural loess, considering the influence of initial moisture content, is established under the framework of critical state theory.

(4) The prediction function of the established constitutive model is realized using a MATLAB numerical tool. The good agreement between the prediction results of the model and the test results has validated the rationality of the established constitutive model in simulating the structure and softening characteristics of loess. The new

parameters introduced into the model are analyzed. The results show that the introduced parameters only cause influence in the deformation process, whereas they do not affect the final state of loess.

Reference

[1] CHEN Zheng-han, XU Zhen-hong, LIU Zu-dian. Some problems about loess collapse[J]. China Civil Engineering Journal, 1986, 3: 86−94.

[2] GE Miao-miao, LI Ning, SHENG Dai-chao, et al. Experimental investigation of microscopic deformation mechanism of unsaturated compacted loess under hydraulic coupling conditions[J]. Rock and Soil Mechanics, 2021, 42(9): 2437−2448.

[3] WENG X L, SUN Y F, ZHANG Y W, et al. Physical modeling of wetting-induced collapse of shield tunneling in loess strata[J]. Tunnelling and Underground Space Technology, 2019, 90: 208−219.

[4] MI Weng-jing, ZHANG Ai-jun, REN Wen-yuan, et al. Study on method of reducing loess subsidence by weight reduction and replacement filling of light soil[J]. Journal of Hydraulic Engineering, 2021, 52(1): 51−61.

[5] LIU M D, CARTER J P. A structured Cam clay model[J]. Canadian Geotechnical Journal, 2002, 39(1): 1313−1332.

[6] LIU M D, CARTER J P, DESAI C S. Modeling compression behavior of structured geomaterials[J]. International Journal of Geomechanics, 2003, 3(2): 191−204.

[7] KAVVADAS M, AMOROSI A. A constitutive model for structured soils[J]. Géotechnique, 2000, 50(3): 263−273.

[8] BAUDET B, STALLEBRASS, S. A constitutive model for structured clays[J]. Géotechnique, 2004, 54(4): 269−278.

[9] ZHU Xian-yang, YAO Yang-ping. A UH constitutive model for structured soils[J]. Rock and Soil Mechanics, 2015, 36(11): 3101−3110, 3228.

[10] KATTI D R, DESAI C S. Modeling and testing of cohesive soil using disturbed state concept[J]. Journal of Engineering Mechanics, 1995, 121(5): 648−658.

[11] CHEN Cun-li, HU Zai-qiang, GAO Peng. Research on relationship between structure and deformation property of intact loess[J]. Rock and Soil Mechanics, 2006, 27(11): 1891−1896.

[12] CHEN Cun-li, GAO Peng, HE Jun-fang. Equivalent linear model of intact loess considering structural effect[J]. Chinese Journal of Geotechnical Engineering, 2007, 29(9): 1330−1336.

[13] SHAO Sheng-jun, ZHOU Fei-fei, LONG Ji-yong. Structural properties of loess and its quantitative parameter[J]. Chinese Journal of Geotechnical Engineering, 2004, 26(4): 531−536.

[14] LUO Ya-sheng, XIE Ding-yi, SHAO Sheng-jun, et al. Structural parameter of soil under complex stress conditins[J]. Chinese Journal of Rock Mechanics and Engineering, 2004, 23(24): 4248−4251.

[15] XIE Ding-yi, QI Ji-lin. Soil structure characteristics and new approach in research on its quantitative parameter[J]. Chinese Journal of Geotechnical Engineering, 1999, 21(6): 651−656.

[16] DENG Guo-hua, SHAO Sheng-jun, YU Fang-tao. Modified Cam-clay model of structured loess[J]. Chinese Journal of Geotechnical Engineering, 2012, 34(5): 834−841.

[17] FANG Xiang-wei, LI Yang-yang, SHEN Chun-ni, et al. Constitutive model of unsaturated intact Q2 loess based on disturbed state concept[J]. Journal of Logistical Engineering University, 2017, 33(4): 1−8.

[18] ZHANG Yu-wei, WENG Xiao-lin, SONG Zhan-ping, et al. A modified Cam-clay model for structural and anisotropic loess[J]. Rock and Soil Mechanics, 2019, 40(3): 1030−1038.

[19] DANG Jin-qian, HAO Yue-qing. Effect of water content on the structure strength of loess[J]. Journal of Water Resources and Water Engineering, 1998, 9(2): 15−19.

[20] CAI Guo-qing, ZHANG Ce, HUANG Zhe-wen, et al. Experimental study on influences of moisture content on shear strength of unsaturated loess[J]. Chinese Journal of Geotechnical Engineering, 2020, 42(Suppl.2): 32−36.

[21] CHEN Cun-li, ZHANG Deng-fei, ZHANG Jie, et al. Compression and wetting deformation behavior of intact loess under isotropic stress[J]. Chinese Journal of Rock Mechanics and Engineering, 2017, 36(7): 1736−1747.

[22] HE Jun-fang. Research on constitutive relation of intact loess considering complex stress path[D]. Xi'an: Xi'an University of Technology, 2008.

[23] ROSCOE K H, SCHOFIELD A N, THURAIRAJAH A. Yielding of clays in states wetter than critical[J]. Géotechnique, 1963, 13(3): 211−240.

[24] SUN De-an, XU Qian-lei, CHEN Bo, et al. Mechanical behavior of unsaturated intact loess over a wide suction range[J]. Chinese Journal of Geotechnical Engineering, 2020, 42(9): 1586−1592.

[25] HU Zai-qiang, ZHANG Teng, ZHU Yi-yun, et al. Elastoplastic softening constitutive model of unsaturated loess[J]. Rock and Soil Mechanics, 2006, 27(Suppl.2): 1103−1106.

[26] DENG Le-juan. Constitutive model of structure loess[D]. Xi'an: Chang'an University, 2018.

[27] CHU Feng, SHAO Sheng-jun. Experimental study on constitutive model of structural Q3 loess in Longdong area based on concept of disturbance state[J]. Chinese Journal of Rock Mechanics and Engineering, 2018, 37(9): 2180−2188.

[28] BEEN K, JEFFERIES M G. A state parameter for sands[J]. Géotechnique, 1995, 35(1): 99−112.